THE ANALYSIS OF AN ILL-POSED PROBLEM USING MULTISCALE RESOLUTION AND SECOND ORDER ADJOINT TECHNIQUES

A.K. Alekseev(1)
Dept. of Aerodynamics and Heat Transfer
RSC "ENERGIA"
Korolev(Kaliningrad), Moscow Region
141070, RUSSIA

and

I. Michael Navon (2)

(2) Department of Mathematics and S.C.R.I.

Florida State University

Tallahassee, FL 32306-4130
USA

Keywords: second order adjoint problem, Ill-Posed problem, regularization, wavelets and adjoint parameter estimation.

Abstract

A wavelet regularization approach is presented for dealing with an ill-posed problem of adjoint parameter estimation applied to estimating inflow parameters from down flow data

in an inverse convection case applied to the two-dimensional parabolized Navier Stokes equations in the limit of large Reynolds numbers. The wavelet method provides a decomposition into two subspaces, by identifying both a well posed as well as an ill-posed subspace, the scale of which is determined by finding the minimal eigenvalues of the Hessian of a cost functional measuring the lack of fit between model prediction and observed parameters. The control space is transformed into a wavelet space. The Hessian of the cost is obtained either by a discrete differentiation of the gradients of the cost derived from the first order adjoint or by using the full second order adjoint. The minimum eigenvalues of the Hessian are obtained either by employing a shifted iteration method [1] or by using the Rayleigh quotient. The numerical results obtained show the usefulness and applicability of this algorithm if the Hessian minimal eigenvalue is greater or equal to the square of the data error dispersion, in which case the problem can be considered as well posed (i.e. regularized). If the regularization fails, i.e. the minimal Hessian eigenvalue is less than the square of the data error dispersion for the problem, the following wavelet scale should be neglected, followed by another algorithm iteration. The use of wavelets also allowed computational efficiency due to reduction of the control dimension obtained by neglecting the small-scale wavelet coefficients.

1. Introduction

The method of well-posed subspace determination using multi-scale (wavelet) approach was proposed in [2] for the solution of ill-posed problems. This algorithm is significantly faster than the method of optimal decomposition of control space into "well-posed" and "ill-posed" subspaces based on the total set of eigenvalues. Nevertheless, the approach in [2] is based on the direct search of eigenvalues and eigenvectors of an explicitly defined linear operator (more precisely, the product of forward and adjoint operators A*A). As an alternative we consider applying here an algorithm for finding the minimum eigenvalue of the Hessian of the cost functional based on the second order adjoint approach presented in [3] to a nonlinear problem in the form of a system of coupled PDE's.

The present paper describes an algorithm for determining a well-posed subspace using elements of both approaches presented in [2] and [3]. The choice of the scale of wavelet transformation is determined by performing a subsequent search for the minimum eigenvalues of a Hessian obtained by considering the first and second order adjoint for a parabolized Navier-Stokes equations model.

The present paper is organized as follows. In Section 2 we present the multiscale regularization approach for the ill-posed problem of adjoint parameter estimation, based on work of Liu et al. [2] along with use of the Fisher informational matrix for estimating the degree of the problem ill-posedness, based on work of Alifanov et al. [5].

Section 3 consists of a short presentation of first and second order adjoint methods for inverse convection problems, followed in Section 4 by the presentation of the first and second order adjoint of the parabolized Navier-Stokes equations as well as the explicit formulation of the cost functional to be minimized for optimal parameter estimation.

Section 5 consists of a brief presentation of the Lagrangian as a first step in the derivation of full expressions for the first and second order adjoint model.

Section 6 describes in detail the tangent linear and Lagrangian variation as a function of the control parameters for the parabolized Navier Stokes equations.

Section 7 presents the first order adjoint model equations followed in Section 8 by the derivation of the second order adjoint. Having in place the forward, tangent linear, first and second order adjoint models we proceed to calculate the spectrum bounds of the Hessian of the cost functional with respect to the control variables. This is done in Section 9 using a Rayleigh quotient and a calculation of the minimal eigenvalues by a shifted iteration method. Results of the optimal parameter estimation using the wavelet regularization procedure with different scales of wavelet transformation are presented for increasing Reynolds numbers and using different scales of regularization related to the wavelet transformation. The parameters were initially rendered ill-posed by perturbing them with a data error. Numerical tests show that the new algorithm performs successfully both in estimating and regularizing inflow parameters related to the inverse convection problem described by the parabolized Navier Stokes equations and that the Hessian minimal eigenvalue increases with increasing Reynolds numbers as well as with the increase in the wavelet scale.

Section 10 consists of brief conclusions and a succinct presentation of the multiscale regularization algorithm employed.

2. Multiscale regularization

Algorithms for ill-posed problems may be often reduced to the solution of ill-conditioned system of linear equations. The ill-conditioned operator may be represented in diagonal form using a singular value decomposition. Some eigenvalues of this operator may be zero or very close to zero. The solution may then be searched in the subspace of those eigenvectors whose eigenvalues are greater than some prescribed value [4]. This method may be viewed as a variant of Occam's regularization procedure where the "simplest" solution is defined as one composed of a minimum number of eigenvectors with large eigenvalues.

We define boundary functions for subspace U⊂V (V- being the control functions' space):

$$B_{\inf}(U) = \inf \frac{\|AX\|}{\|X\|}; B_{\sup}(U) = \sup \frac{\|AX\|}{\|X\|};$$

Using singular value decomposition, we can define V as a sum V= $V_\varepsilon^+ + V_\varepsilon^-$, such that $B_{inf}(V_\varepsilon^+)>\varepsilon$, $B_{sup}(V_\varepsilon^-)<\varepsilon$. V_ε^+ is spanned by eigenvectors $\{v_1, v_2 \ldots v_L\}$ while V_ε^- by $\{v_{L+1}, v_{L+2} \ldots v_N\}$. Herein, the eigenvectors are ordered according to eigenvalues' magnitudes $\lambda_L>\varepsilon>\lambda_{L+1}$. We may

numerical stability. This approach implies the calculation of all eigenvalues and eigenvectors, which is a computationally intensive task.

Singular value decomposition may be replaced by multiscale (wavelet) decomposition [2]. We may construct the sequence of subspaces with decreasing B_{inf}. This allows us to find two (suboptimal) subspaces U_ε^- , U_ε^+ : $B_{inf}(U_\varepsilon^+)>\varepsilon$. Multiscale resolution is based on the sequence of subspaces:

$V_0 \subset V_1 \subset V_2 \ldots \subset V_j \subset V$.

$V_j = V_0 \oplus W_0 \oplus W_1 \oplus W_{j-1}$

$V = V_0 \oplus W_0 \oplus W_1 \oplus W_j \oplus \ldots.$

The space V may then be decomposed into two subspaces for every scale *j*.

$$V = V_j + V_j^{\perp} , \; V_j^{\perp} = W_j + W_{j+1} + \ldots$$

Work by [2] demonstrates (for Haar basis), that $B_{sup}(V_j^{\perp}) \le C \cdot 2^{-j/2}$ and for every ε we can find *j* such that $B_{sup}(V_j^{\perp}) \le \varepsilon$. Thus, wavelet transformation provides an ordering of subspaces $V_j^{\perp}$ according to the scale *j* and the minimal eigenvalues. There is no similar proof for $B_{inf}(V_j)$ (although such ordering seems to be quite natural). So, our numerical tests are performed in order to estimate λ_{min} for the sequence V_j depending on the scale *j*. According to [2], the discrete wavelet transformation (pyramidal algorithm) is used for approximation of the control functions

$$f(x) = \sum_{j=0}^{N} \sum_{k=0}^{2^j - 1} a_{2^j+1} W(2^j - k)$$

Where *j* – is the scale, *k* –translation, *N* is a number of controls. The Daubechies-20 [6] transform was used as it is

Haar transformation. Numerical tests confirmed a decrease of λ_{min} (V_j) depending on the scale j.

An approach using the Fisher information matrix (approximating the Hessian in the vicinity of solution) is described in [5] for estimation of problem ill-posedness.

Given the discrepancy (cost functional) $\varepsilon(u) = \sum_i (f_i^{obs} - f_i(u))^2$ the Hessian assumes the form

$$H_{jk} = \frac{\partial^2 \varepsilon}{\partial u_{jk}} = \sum_i \frac{\partial f_i}{\partial u_j}\frac{\partial f_i}{\partial u_k} - 2\sum_i (f_i^{obs} - f_i)\frac{\partial^2 f_i}{\partial u_j \partial u_k};$$

Let $S_{ij} = \frac{\partial f_i}{\partial u_j}$ - sensitivity matrix (rectangular) and

$M_{ij} = \frac{\partial f_k}{\partial u_i}\frac{\partial f_k}{\partial u_j}$ - informational matrix (square). When divided by data error dispersion the Fisher matrix is defined by

$$M_{ij} = \sum_k \frac{1}{\sigma_k^2}\frac{\partial f_k}{\partial u_i}\frac{\partial f_k}{\partial u_j}$$

The inverse matrix $D=M^{-1}$ is a dispersion matrix of the control parameters' error u_j. The magnitude of the Fisher informational matrix minimal eigenvalue compared with data error $\lambda_{min} \approx \sigma^2$ may be used for estimating the problem ill-posedness [5]. The calculation of the informational matrix is based on the system of sensitivity equations, which is more time consuming compared with the adjoint approach.

3. Adjoint Problems of the First and Second Order

The solution of the adjoint problem used for gradient calculation is the standard approach used for the inverse convection problems [3,7]. The action of Hessian may be calculated by using second order adjoint approach [3]. In accordance with [3] we consider here the general scheme for second order adjoint problem. Herein X- denotes the marching coordinate (time analogue), f - variables.

Forward problem

$$\frac{df}{dX} = F(f);\ f(0)=U;\ \varepsilon(U)=\frac{1}{2}\int_0^Y \|Cf - f_{obs}\|^2 dY; \tag{1}$$

First order adjoint problem

$$\frac{d\Psi}{dX}+\frac{\partial F}{\partial f}^T \Psi = C^T(Cf - f_{obs});\ \Psi(1)=0;\ \nabla\varepsilon(U)=-\Psi(0); \tag{2}$$

Tangent problem

$$\frac{d\,\overset{|}{f}}{dX} = \frac{\partial F}{\partial f}\overset{|}{f};\ \overset{|}{f}(0)=u; \tag{3}$$

Second order adjoint problem (tangent to first order adjoint)

$$\frac{d\,\overset{|}{\Psi}}{dX}+\frac{\partial^2 F}{\partial f^2}\overset{|}{f}\,\Psi+\frac{\partial F}{\partial f}^T\overset{|}{\Psi}=C^T C\overset{|}{f}; \tag{4}$$

$$\overset{|}{\Psi}(1)=0;\quad \overset{|}{\varepsilon}(U)=H(U)u=-\overset{|}{\Psi}(0);$$

Thus, the Hessian action on the vector ***u*** may be obtained by sequentially solving Eqs. (1), (2), and (3), (4) (all about the forward problem from a computer resources viewpoint).

Numerical differentiation using the expression *Hdu=(grad(u+adu)-grad(u))/a* requires also four solutions of this type of problem but is somewhat less accurate.

In the following, we consider the scheme (1-4) for the two-dimensional parabolized Navier Stokes equations, given by:

4. First and Second Order Adjoint Problems for Parabolized Navier-Stokes Equations

We consider here the problem estimation of the inflow parameters $\boldsymbol{u}=f_\infty(Y)=(\rho(Y),U(Y),V(Y),T(Y))$ from outflow measurements (Fig. 1). The flow is two-dimensional supersonic laminar one governed by the parabolized Navier Stokes equations:

$$\frac{\partial(\rho U)}{\partial X}+\frac{\partial(\rho V)}{\partial Y}=0 \qquad (5)$$

$$U\frac{\partial U}{\partial X}+V\frac{\partial U}{\partial Y}+\frac{1}{\rho}\frac{\partial P}{\partial X}=\frac{1}{\mathrm{Re}\,\rho}\frac{\partial^2 U}{\partial Y^2} \qquad (6)$$

$$U\frac{\partial V}{\partial X}+V\frac{\partial V}{\partial Y}+\frac{1}{\rho}\frac{\partial P}{\partial Y}=\frac{4}{3\rho\,\mathrm{Re}}\frac{\partial^2 V}{\partial Y^2} \qquad (7)$$

$$U\frac{\partial e}{\partial X}+V\frac{\partial e}{\partial Y}+(\kappa-1)e\left(\frac{\partial U}{\partial X}+\frac{\partial V}{\partial Y}\right)=\frac{1-\kappa}{\rho}\frac{1}{\mathrm{Re}\,\mathrm{Pr}}\frac{\partial^2 e}{\partial Y^2}+\frac{4}{3\mathrm{Re}}\left(\frac{\partial U}{\partial Y}\right)^2 \qquad (8)$$

where $e=C_v T=R/(\kappa-1)T$; $P=(\kappa-1)\rho e$,

$(X,Y)\in Q=(0<X<1;0<Y<1)$;

The boundary conditions of undisturbed external flow (9) are used on the boundaries $Y=0$, $Y=1$.

$$f(0,Y)=f_\infty(Y);\ f(X,1)=f_\infty(1);\ f(X,0)=f_\infty(0); \qquad (9)$$

We search for $f_\infty(Y)=(\rho(Y),U(Y),V(Y),e(Y))$ using outflow data (Fig. 1) by minimizing discrepancy

$$\varepsilon(f_\times(Y))=\int_Y (f_{obs}(X,Y)-f(X,Y))^2\,\delta(X-X_m)\,\delta(Y-Y_m)\,dX\,dY \qquad (10)$$

5. The Lagrangian

According to [3,5,7] we define the Lagrangian using the weak form of Eqs. (5-8) and the discrepancy (10).

$$\varepsilon_o(f_\infty(Y)) = \varepsilon(f_\infty(Y)) + \iint_{X\,Y}\left(\frac{f(\rho U)}{fX}+\frac{f(\rho V)}{fY}\right)\Psi_\rho(X,Y)dXdY +$$

$$+\iint_{X\,Y}\left(U\frac{fU}{fX}+V\frac{fU}{fY}+\frac{1}{\rho}\frac{fP}{fX}-\frac{1}{Re\,\rho}\frac{f^2U}{fY^2}\right)\Psi_U(X,Y)dXdY +$$

$$+\iint_{X\,Y}\left(U\frac{fV}{fX}+V\frac{fV}{fY}+\frac{1}{\rho}\frac{fP}{fY}-\frac{4}{3\,Re\,\rho}\frac{f^2V}{fY^2}\right)\Psi_V(X,Y)dXdY +$$

$$+\iint_{X\,Y}\left(U\frac{fe}{fX}+V\frac{fe}{fY}+(\kappa-1)e\left(\frac{fU}{fX}+\frac{fV}{fY}\right)-\frac{\kappa}{\rho\,Re\,Pr}\frac{f^2e}{fY^2}-\frac{4}{3\,Re\,\rho}\left(\frac{fU}{fY}\right)^2\right)\Psi_e(X,Y)dXdY; \quad (11)$$

We consider $(\Psi_\rho(X,Y), \Psi_U(X,Y), \Psi_V(X,Y), \Psi_e(X,Y)) \in H^{1,2}(Q)$, where $H^{1,2}(Q)$ is a Hilbert space of first and second order distributions.

6. Tangent Linear problem and Lagrangian Variation

The tangent linear problem should be stated for determination of the Lagrangian's (11) variation as a function of the control parameters' variation. We disturb the boundary condition (9)

$$\Delta f(0,Y) = \Delta f_\infty(Y) \quad (12)$$

and obtain corresponding variations of $\Delta\rho, \Delta U, \Delta V, \Delta e$ in (5-8) by subtracting the undisturbed variables.

$$U^{f(\Delta\rho)} + \rho^{f(\Delta U)} + \rho^{f(\Delta V)} + V^{f(\Delta\rho)} +$$

$$\Delta\rho\frac{fU}{fX}+\Delta U\frac{f\rho}{fX}+\Delta\rho\frac{fV}{fY}+\Delta V\frac{f\rho}{fY}=0 \qquad (13)$$

$$U\frac{f\Delta U}{fX}+\Delta U\frac{fU}{fX}+\Delta V\frac{fU}{fY}+V\frac{f\Delta U}{fY}-\frac{1}{\rho\,\mathrm{Re}}\frac{f^2\Delta U}{fY^2}+\frac{\Delta\rho}{\rho^2\,\mathrm{Re}}\frac{f^2U}{fY^2}-$$
$$-\frac{\Delta\rho}{\rho^2}\frac{fP}{fX}+\frac{(\kappa-1)}{\rho}\Delta\rho\frac{fe}{fX}+e\frac{f\Delta\rho}{fX}+\rho\frac{f\Delta e}{fX}+\Delta e\frac{f\rho}{fX}=0$$

(14)

$$U\frac{f\Delta V}{fX}+\Delta U\frac{fV}{fX}+\Delta V\frac{fV}{fY}+V\frac{f\Delta V}{fY}-\frac{4}{3\rho\,Re}\frac{f^2\Delta V}{fY^2}+\frac{4\Delta\rho}{3\rho^2\,Re}\frac{f^2V}{fY^2}-$$
$$-\frac{\Delta\rho}{\rho^2}\frac{fP}{fY}+\frac{(\kappa-1)}{\rho}\Delta\rho\frac{fe}{fY}+e\frac{f\Delta\rho}{fY}+\rho\frac{f\Delta e}{fY}+\Delta e\frac{f\rho}{fY}=0$$

(15)

$$U\frac{f\Delta e}{fX}+\Delta U\frac{fe}{fX}+\Delta V\frac{fe}{fY}+V\frac{f\Delta e}{fY}+(\kappa-1)\Delta e\left(\frac{fU}{fX}+\frac{fV}{fY}\right)+(\kappa-1)e\left(\frac{f\Delta U}{fX}+\frac{f\Delta V}{fY}\right)-$$
$$-\frac{1}{\rho}\frac{\kappa}{Re\,Pr}\frac{f^2\Delta e}{fY^2}-\frac{\kappa}{Re\,Pr}\frac{\Delta\rho}{\rho}\frac{f^2e}{fY^2}+\frac{8}{3\,Re}\left(\frac{f\Delta U}{fY}\left(\frac{fU}{fY}\right)-\frac{\Delta\rho}{\rho}\frac{4}{3\,Re}\left(\frac{fU}{fY}\right)^2\right)=0;$$

(16)

$$\Delta f(0,Y)=\Delta f_\infty(Y);\ \Delta f(X,1)=\Delta f_\infty(1);\qquad (17)$$
$$\Delta f(X,0)=\Delta f_\infty(0);$$

We now form the Lagrangian variation (11) with respect to $\Delta\rho,\Delta U,\Delta V,\Delta e$. By subtracting the undisturbed solution and retaining only first order terms we get

$$\Delta\varepsilon_o(f_\times(Y))=\Delta\varepsilon(f_\times(Y))+$$

$$+\int_Y\int_X\left(U\frac{f(\Delta\rho)}{fX}+\rho\frac{f(\Delta U)}{fX}+\rho\frac{f(\Delta V)}{fY}+V\frac{f(\Delta\rho)}{fY}\right)\Psi_\rho\,dX\,dY+$$

$$+\int_Y\int_X \overline{\Delta\rho}\frac{fU}{fX}+\Delta U\frac{f\rho}{fX}+\Delta\rho\frac{fV}{fY}+\Delta V\frac{f\rho}{fY}\Psi_\rho dXdY+$$

$$+\int_X\int_Y \overline{U}\frac{f\Delta U}{fX}+\Delta U\frac{fU}{fX}+\Delta V\frac{fU}{fY}+V\frac{f\Delta U}{fY}-\frac{1}{\rho\,\mathrm{Re}}\frac{f^2\Delta U}{fY^2}+\frac{\Delta\rho}{\rho^2\,\mathrm{RE}}\frac{f^2U}{fY^2}-\frac{\Delta\rho}{\rho^2}\frac{fP}{fX}+$$
$$+\frac{\kappa-1}{\rho}\overline{\Delta\rho}\frac{fe}{fX}+e\frac{f\Delta\rho}{fX}+\rho\frac{f\Delta e}{fX}+\Delta e\frac{f\rho}{fX}\Psi_U(X,Y)dXdY+$$

$$+\int_X\int_Y \overline{U}\frac{f\Delta V}{fX}+\Delta U\frac{fV}{fX}+\Delta V\frac{fV}{fY}+V\frac{f\Delta V}{fY}-\frac{4}{3\rho\,\mathrm{Re}}\frac{f^2\Delta V}{fY^2}+\frac{4\Delta\rho}{3\rho^2\,\mathrm{Re}}\frac{f^2V}{fY^2}-$$

$$-\frac{\Delta\rho}{\rho^2}\frac{fP}{fY}+\frac{\kappa-1}{\rho}\overline{\Delta\rho}\frac{fe}{fY}+e\frac{f\Delta\rho}{fY}+\rho\frac{f\Delta e}{fY}+\Delta e\frac{f\rho}{fY}\Psi_V(X,Y)dXdY+$$
$$+\int_X\int_Y \overline{U}\frac{f\Delta e}{fX}+\Delta U\frac{fe}{fX}+\Delta V\frac{fe}{fY}+V\frac{f\Delta e}{fY}+(\kappa-1)\Delta e\overline{\frac{fU}{fX}+\frac{fV}{fY}}+(k-1)e\overline{\frac{f\Delta U}{fX}+\frac{f\Delta V}{fY}}-$$

$$-\frac{1}{\rho\,\mathrm{Re}}\overline{\frac{\kappa}{\mathrm{Pr}}\frac{f^2\Delta e}{fY^2}}-\frac{\kappa}{\mathrm{Pr}}\frac{\Delta\rho}{\rho}\frac{f^2e}{fY^2}+\frac{8}{3}\overline{\frac{f\Delta U}{fY}}\overline{\frac{fU}{fY}}-\frac{\Delta\rho}{\rho}\frac{4}{3}\overline{\frac{fU}{fY}}^2\Psi_e(X,Y)dXdY$$

(18)

After rearranging the terms with $\Delta\rho,\Delta U,\Delta V,\Delta e$ we obtain:

$$\Delta\varepsilon_0(f_\times(Y)=$$

$$\int_X\int_Y \overline{\overline{U}}\frac{f(\Delta\rho)}{fX}+V\frac{f(\Delta\rho)}{fY}\Psi_\rho(X,Y)+$$
$$+\overline{\frac{fU}{fX}+\frac{fV}{fY}}\Psi_\rho\Delta\rho+$$
$$+\frac{\kappa-1}{\rho}\overline{\frac{f(\Delta\rho)}{fY}}e+\Delta\rho\frac{fe}{fY}\Psi_V+\frac{\kappa-1}{\rho}\overline{\frac{f(\Delta\rho)}{fX}}e+\Delta\rho\frac{fe}{fX}\Psi_U+$$

$$+\frac{\Delta\rho}{\rho^2}\overline{-\frac{fP}{fX}}+\frac{1}{\mathrm{Re}}\frac{f^2U}{fY^2}\Psi_U+\frac{\Delta\rho}{\rho^2}\overline{-\frac{fP}{fY}}+\frac{4}{3\mathrm{Re}}\frac{f^2V}{fY^2}\Psi_V+$$
$$+\frac{\Delta\rho}{\rho^2}\overline{\frac{\kappa}{\mathrm{RePr}}\frac{f^2e}{fY^2}}+\frac{4}{3\mathrm{Re}}\overline{\frac{fU}{fY}}^2\Psi_e dXdY+$$

$$+\int_X\int_Y \overline{\overline{U}}\frac{f\Delta U}{fX}+\Delta U\frac{fU}{fX}+V\frac{f\Delta U}{fY}-\frac{1}{\rho\,\mathrm{Re}}\frac{f^2\Delta U}{fY^2}\Psi_U(X,Y)+$$
$$+\frac{f\rho}{fX}\Psi_\rho\Delta U+$$

$$+\rho\frac{f\Delta U}{fX}\Psi_\rho+\Delta U\frac{fV}{fX}\Psi_V+\Delta U\frac{fe}{fX}\Psi_e+(\kappa-1)e\frac{f\Delta U}{fX}\Psi_e-$$
$$-\frac{8}{3\,Re}\frac{fU}{fY}\frac{f\Delta U}{fY}\Psi_e\sqrt{\downarrow}dXdY+$$

$$+\overline{\overline{U}}\frac{f\Delta V}{fX}+\Delta V\frac{fV}{fY}+V\frac{f\Delta V}{fY}-\frac{4}{3\rho\,\mathrm{Re}}\frac{f^2\Delta V}{fY^2}\sqrt{\downarrow}\Psi_V(X,Y)+$$
$$+\Delta V\frac{fU}{fY}\Psi_U+\rho\frac{f\Delta V}{fY}\Psi_\rho+\Delta V\frac{fe}{fY}\Psi_e+(\kappa-1)e\frac{f\Delta V}{fY}\Psi_e\sqrt{\downarrow}dXdY+$$
$$+\frac{f\rho}{fY}\Psi_\rho\Delta V+$$
$$+\overline{\overline{U}}\frac{f\Delta e}{fX}+V\frac{f\Delta e}{fY}+(\kappa-1)\Delta e\frac{fU}{fX}+\frac{fV}{fY}\sqrt{\downarrow}-\frac{\kappa}{\rho\,\mathrm{Re}\,\mathrm{Pr}}\frac{f^2\Delta e}{fY^2}\sqrt{\downarrow}\Psi_e(X,Y)+$$
$$+\frac{\kappa-1}{\rho}\frac{f\rho}{fY}\Delta e+\rho\frac{f\Delta e}{fY}\sqrt{\downarrow}\Psi_V+\frac{\kappa-1}{\rho}\frac{f\rho}{fX}\Delta e+\rho\frac{f\Delta e}{fX}\sqrt{\downarrow}\Psi_U\sqrt{\downarrow}dXdY$$

(19)

We integrate this equation by parts and taking into account boundary conditions for $\Delta\rho,\Delta U,\Delta V,\Delta e$, respectively, we get

$$\Delta\varepsilon_o(f_\times(Y))=$$

Terms with $\Delta\rho$:

$$\int_Y\Psi_\rho U\Delta\rho dY\Big|_{X=0}^{X=1}-\int_Y\int_X\frac{f(U\Psi_\rho)}{fX}\Delta\rho dXdY+$$
$$+\int_X\Psi_\rho V\Delta\rho dX\Big|_{Y=0}^{Y=1}-\int_Y\int_X\frac{f(V\Psi_\rho)}{fY}\Delta\rho dXdY+$$
$$+\int_Y\int_X\left(\frac{fU}{fX}+\frac{fV}{fY}\sqrt{\downarrow}\right)\Psi_\rho\Delta\rho dXdY+$$
$$(\kappa-1)\int_X\Psi_V e\rho^{-1}\Delta\rho dX\Big|_{Y=0}^{Y=1}-(\kappa-1)\int_Y\int_X\frac{f(\Psi_V e/\rho)}{fY}\Delta\rho dXdY+$$
$$+(\kappa-1)\int_Y\Psi_U e/\rho\Delta\rho dY\Big|_{X=0}^{X=1}-(\kappa-1)\int_Y\int_X\frac{f(\Psi_U e/\rho)}{fX}\Delta\rho dXdY+$$
$$+\int_Y\int_X\left(\frac{\kappa-1}{\rho}\frac{fe}{fY}\Psi_V+\frac{fe}{fX}\Psi_U\sqrt{\downarrow}\right)\Delta\rho dXdY+$$

$$+\int_Y\int_X \frac{1}{\rho^2}\left(-\frac{\partial P}{\partial X}+\frac{1}{\mathrm{Re}}\frac{\partial^2 U}{\partial Y^2}\right)\Psi_U+\left(-\frac{\partial P}{\partial Y}+\frac{4}{3\mathrm{Re}}\frac{\partial^2 V}{\partial Y^2}\right)\Psi_V+$$

$$+\left(\frac{\kappa}{\mathrm{Re}\,\mathrm{Pr}}\frac{\partial^2 e}{\partial Y^2}+\frac{4}{3\,\mathrm{Re}}\left(\frac{\partial U}{\partial Y}\right)^2\right)\Psi_e\,\Delta\rho\,dXdY-$$

$$-\int_X\int_Y 2(\rho_{obs}(X,Y)-\rho(X,Y))\Delta\rho(X,Y)\delta(X-X_m)\delta(Y-Y_m)dXdY+$$

terms with ΔU:

$$+\int_Y \Psi_U U\Delta U dY\Big|_{X=0}^{X=1}-\int_Y\int_X \frac{\partial(U\Psi_U)}{\partial X}\Delta U dXdY+$$

$$+\int_X \Psi_U V\Delta U dX\Big|_{Y=0}^{Y=1}-\int_Y\int_X \frac{\partial(V\Psi_U)}{\partial Y}\Delta U dXdY+$$

$$+\int_Y \Psi_\rho \rho\Delta U dY\Big|_{X=0}^{X=1}-\int_Y\int_X \frac{\partial(\Psi_\rho\rho)}{\partial X}\Delta U dXdY+$$

$$+\int_Y\int_X \Psi_\rho\frac{\partial\rho}{\partial X}\Delta U dXdY+$$

$$+\int_Y\int_X\left(+\frac{\partial U}{\partial X}\Psi_U+\frac{\partial V}{\partial X}\Psi_V+\frac{\partial e}{\partial X}\Psi_e\right)\Delta U dXdY+$$

$$+\int_Y \Psi_e\frac{P}{\rho}\Delta U dY\Big|_{X=0}^{X=1}-\int_Y\int_X \frac{\partial}{\partial X}\Psi_e\frac{P}{\rho}\Delta U dXdY+$$

$$-\frac{8}{3\,\mathrm{Re}}\int_X \Psi_e\frac{\partial U}{\partial Y}\Delta U\,?dX\Big|_{Y=0}^{Y=1}+\frac{8}{3\,\mathrm{Re}}\int_Y\int_X \frac{\partial}{\partial Y}\Psi_e\frac{\partial u}{\partial Y}\Delta U dXdY-$$

$$-\int_X \frac{1}{\rho\,\mathrm{Re}}\frac{\partial\Delta U}{\partial Y}\Psi_U dX\Big|_{Y=0}^{Y=1}+\int_X\frac{\partial}{\partial y}\frac{1}{\rho\,\mathrm{Re}}\Psi_U\Delta U dY\Big|_{Y=0}^{Y=1}-$$

$$-\int_Y\int_X \frac{\partial^2}{\partial y^2}\frac{\mu}{\rho}\Psi_U\Delta U dXdY-$$

$$-\int_X\int_Y 2(U_{obs}(X,Y)-U(X,Y))\Delta U(X,Y)\delta(X-X_m)\delta(Y-Y_m)dXdY+$$

terms with ΔV:

$$+\int_Y \Psi_V U\Delta V dY\Big|_{X=0}^{X=1}-\int_Y\int_X \frac{\partial(U\Psi_V)}{\partial X}\Delta V dXdY+$$

$$+\int_X \Psi_V V\Delta V dX\Big|_{Y=0}^{Y=1}-\int_Y\int_X \frac{\partial(V\Psi_V)}{\partial Y}\Delta V dXdY+$$

$$+\int_Y\int_X\left(+\frac{\partial V}{\partial Y}\Psi_V+\frac{\partial U}{\partial Y}\Psi_U+\frac{\partial e}{\partial Y}\Psi_e\right)\Delta V dXdY+$$

$$+\int_X \overline{\Psi_\rho}\rho + \frac{P}{\rho}\Psi_e \sqrt{\Delta V}dX\Big|_{Y=0}^{Y=1} - \int_Y \int_X \frac{f}{fY}\overline{\Psi_\rho}\rho + \frac{P}{\rho}\Psi_e \sqrt{\Delta V}dXdY +$$

$$+\int_Y \int_X \Psi_\rho \frac{f\rho}{fY}\Delta V dXdY +$$

$$-\int_X \frac{4}{3\rho\,\mathrm{Re}}\frac{f\Delta V}{fY}\Psi_V dX\Big|_{Y=0}^{Y=1} + \int_X \frac{f}{fy}\frac{4}{3\rho\,\mathrm{Re}}\Psi_V \sqrt{\Delta V}dX\Big|_{Y=0}^{Y=1} -$$

$$-\frac{4}{3\,Re}\int_Y \int_X \frac{f^2}{fy^2}\frac{1}{\rho}\Psi_V \sqrt{\Delta V}dXdY -$$

$$-\int_X \int_Y 2(V_{obs}(X,Y) - V(X,Y))\Delta V(X,Y)\delta(X - X_m)\delta(Y - Y_m)dXdY +$$

Terms with Δe:

$$\int_Y \Psi_e U\Delta e dY\Big|_{X=0}^{X=1} - \int_Y \int_X \frac{f(U\Psi_e)}{fX}\Delta e dXdY +$$

$$+\int_X \Psi_e V\Delta e dX\Big|_{Y=0}^{Y=1} - \int_Y \int_X \frac{f(V\Psi_e)}{fY}\Delta e dXdY +$$

$$+\int_Y \int_X \frac{\kappa - 1}{\rho}\left(\frac{f\rho}{fY}\Psi_V + \frac{f\rho}{fX}\Psi_U\right)\sqrt{} + (\kappa - 1)\frac{fU}{fX} + \frac{fV}{fY}\sqrt{}\Psi_e \sqrt{\Delta e}?dX?dY +$$

$$+(\kappa - 1)\int_X \Psi_V \Delta e dX\Big|_{Y=0}^{Y=1} - (\kappa - 1)\int_Y \int_X \frac{f}{fY}(\Psi_V)\Delta e dXdY +$$

$$+(\kappa - 1)\int_Y \Psi_U \Delta e dY\Big|_{X=0}^{X=1} - (\kappa - 1)\int_Y \int_X \frac{f}{fX}(\Psi_U)\Delta e dXdY -$$

$$+\int_X \int_Y 2(e_{obs}(X,Y) - e(X,Y))\Delta e(X,Y)\delta(X - X_m)\delta(Y - Y_m)dXdY$$

$$-\int_X \frac{\kappa}{\rho\,\mathrm{Re}\,\mathrm{Pr}}\frac{f\Delta e}{fY}\Psi_e dX\Big|_{Y=0}^{Y=1} + \int_X \frac{f}{fy}\frac{\kappa}{\rho\,\mathrm{Re}\,\mathrm{Pr}}\Psi_e \sqrt{\Delta e}dY\Big|_{Y=0}^{Y=1} -$$

$$-\int_Y \int_X \frac{f^2}{fy^2}\frac{\kappa}{\rho\,\mathrm{Re}\,\mathrm{Pr}}\Psi_e \sqrt{\Delta e}dXdY$$

(20)

We look for $(\Psi_\rho, \Psi_U, \Psi_V, \Psi_e)$ such that $\Delta\varepsilon_0 = \int_Y grad(\varepsilon)\Delta f_\infty(Y)dY$ while all other first order terms vanish .

7. First order adjoint Equations

$$U\frac{\partial\Psi_\rho}{\partial X}+V\frac{\partial\Psi_\rho}{\partial Y}+(\kappa-1)\frac{\partial(\Psi_V e/\rho)}{\partial Y}+(\kappa-1)\frac{\partial(\Psi_U e/\rho)}{\partial X}-$$
$$-\frac{\kappa-1}{\rho}\frac{\partial e}{\partial Y}\Psi_V+\frac{\partial e}{\partial X}\Psi_U\Big|_{\leftarrow\lrcorner}+\frac{1}{\rho^2}\frac{\partial P}{\partial X}-\frac{1}{\rho^2\,\mathrm{Re}}\frac{\partial^2 U}{\partial Y^2}\Big|_{\leftarrow\lrcorner}\Psi_U+\frac{1}{\rho^2}\frac{\partial P}{\partial Y}-\frac{4}{3\mathrm{Re}}\frac{\partial^2 V}{\partial Y^2}\Big|_{\leftarrow\lrcorner}\Psi_V-$$
$$-\frac{1}{\rho^2}\frac{\gamma}{\mathrm{Re}\,\mathrm{Pr}}\frac{\partial^2 e}{\partial Y^2}+\frac{4}{3\mathrm{Re}}\frac{\partial U}{\partial Y}\Big|_{\leftarrow\lrcorner}^{2}\Psi_e+2\left(\rho_{obs}(X,Y)-\rho(X,Y)\right)\delta(X-X_m)\delta(Y-Y_m)=0$$

(21)

$$U\frac{\partial\Psi_U}{\partial X}+\frac{\partial(\Psi_U V)}{\partial Y}+\rho\frac{\partial\Psi_\rho}{\partial X}-\frac{\partial V}{\partial X}\Psi_V+\frac{\partial e}{\partial X}\Psi_e\Big|_{\leftarrow\lrcorner}+\frac{\partial}{\partial X}\frac{P}{\rho}\Psi_e\Big|_{\leftarrow\lrcorner}+$$
$$+\frac{\partial^2}{\partial Y^2}\frac{1}{\rho\,\mathrm{Re}}\Psi_U\Big|_{\leftarrow\lrcorner}-\frac{\partial}{\partial Y}\frac{8}{3\,\mathrm{Re}}\frac{\partial U}{\partial Y}\Psi_e\Big|_{\leftarrow\lrcorner}+$$
$$+2\left(U_{obs}(X,Y)-U(X,Y)\right)\delta(X-X_m)\delta(Y-Y_m)=0 \qquad (22)$$

$$\frac{\partial(U\Psi_V)}{\partial X}+V\frac{\partial\Psi_V}{\partial Y}-\frac{\partial U}{\partial Y}\Psi_U+\frac{\partial e}{\partial Y}\Psi_e\Big|_{\leftarrow\lrcorner}+$$
$$+\rho\frac{\partial\Psi_\rho}{\partial Y}+\frac{\partial}{\partial Y}\frac{P}{\rho}\Psi_e\Big|_{\leftarrow\lrcorner}+\frac{4}{3\mathrm{Re}}\frac{\partial^2}{\partial Y^2}\frac{\Psi_V}{\rho}\Big|_{\leftarrow\lrcorner}+$$
$$+2\left(V_{obs}(X,Y)-V(X,Y)\right)\delta(X-X_m)\delta(Y-Y_m)=0 \qquad (23)$$

$$\frac{\partial(U\Psi_e)}{\partial X}+\frac{\partial(V\Psi_e)}{\partial Y}-\frac{\kappa-1}{\rho}\frac{\partial\rho}{\partial Y}\Psi_V+\frac{\partial\rho}{\partial X}\Psi_U\Big|_{\leftarrow\lrcorner}-(\kappa-1)\frac{\partial U}{\partial X}+\frac{\partial V}{\partial Y}\Big|_{\leftarrow\lrcorner}\Psi_e+$$
$$+(\kappa-1)\frac{\partial\Psi_V}{\partial Y}+(\kappa-1)\frac{\partial\Psi_U}{\partial X}+\frac{\kappa}{\mathrm{Re}\,\mathrm{Pr}}\frac{\partial^2}{\partial Y^2}\frac{\Psi_e}{\rho}\Big|_{\leftarrow\lrcorner}+$$
$$+2\left(e_{obs}(X,Y)-e(X,Y)\right)\delta(X-X_m)\delta(Y-Y_m)=0 \qquad (24)$$

Initial $(X=1)$ and boundary $(Y=0;\ Y=1)$ conditions yield:

$$(U\Psi_\rho+\Psi_U e/\rho)\Big|_{X=1}=0; \qquad \Psi_\rho\Big|_{Y=1}=0; \qquad \Psi_{\rho\,Y=0}=1$$

$$(U\Psi_U+\Psi_\rho+\Psi(\kappa-1)e)\Big|_{X=1}=0 \qquad \Psi_U\Big|_{Y=1}=0;$$

(25)

$$(U\Psi_e + (\kappa-1)\Psi_U)\Big|^{X=1} = 0; \qquad \Psi_e\Big|^{Y=1} = 0; \qquad \Psi|_{e\,Y=0} = 0$$

$$(\Psi_V)\Big|^{x=1} = 0; \qquad \Psi_V\Big|^{Y=1} = 0; \qquad \Psi|_{V\,Y=0} = 0$$

If Eqs. (21-25) are satisfied then

$$\Delta\varepsilon_0(f_\times(Y)) = \int_Y \left(\Psi_e U + (\kappa-1)\Psi_U\right)\Delta e_\times(Y)\Big|_{X=0} dY +$$

$$+ \int_Y \Psi_\rho U + (\kappa-1)\Psi_U e/\rho\,\Delta\rho_\times(Y)\Big|_{X=0} dY +$$

$$+ \int_Y \left(\Psi_U U + \rho\Psi_\rho + (\kappa-1)\Psi_e e\right)\Delta U_\times(Y)\Big|_{X=0} dY + \int_Y \left(\Psi_V U \Delta V_\times(Y)\right)\Big|_{X=0} dY \qquad (26)$$

8. Second Order Adjoint Problem

According to Eq. (4) we can pose the Second Order Adjoint Problem for Q_ρ, Q_U, Q_V, Q_e:

$$U\frac{\partial Q_\rho}{\partial X} + V\frac{\partial Q_\rho}{\partial Y} + (\kappa-1)\frac{\partial(Q_V e/\rho)}{\partial Y} + (\kappa-1)\frac{\partial(Q_U e/\rho)}{\partial X} -$$

$$- \frac{\kappa-1}{\rho}\left(\frac{\partial e}{\partial Y}Q_V + \frac{\partial e}{\partial X}Q_U\right) + \left(\frac{1}{\rho^2}\frac{\partial P}{\partial X} - \frac{1}{\rho^2\,Re}\frac{\partial^2 U}{\partial Y^2}\right)Q_U + \left(\frac{1}{\rho^2}\frac{\partial P}{\partial Y} - \frac{4}{3\,Re}\frac{\partial^2 V}{\partial Y^2}\right)Q_V -$$

$$- \left(\frac{1}{\rho^2}\frac{\gamma}{Re\,Pr}\frac{\partial^2 e}{\partial Y^2} + \frac{4}{3\,Re}\left(\frac{\partial U}{\partial Y}\right)^2\right)Q_e =$$

$$= 2\Delta\rho\,\delta(X - X_m)\delta(Y - Y_m) -$$

$$- \Delta U\frac{\partial\Psi_\rho}{\partial X} - \Delta V\frac{\partial\Psi_\rho}{\partial Y} - (\kappa-1)\frac{\partial(\Psi_V\Delta(e/\rho))}{\partial Y} - (\kappa-1)\frac{\partial(\Psi_U\Delta(e/\rho))}{\partial X} +$$

$$+ \frac{\kappa-1}{\rho}\left(\frac{\partial\Delta e}{\partial Y}\Psi_V + \frac{\partial\Delta e}{\partial X}\Psi_U\right) - \left(\frac{1}{\rho^2}\frac{\partial\Delta P}{\partial X} - \frac{1}{\rho^2\,Re}\frac{\partial^2\Delta U}{\partial Y^2}\right)\Psi_U - \left(\frac{1}{\rho^2}\frac{\partial\Delta P}{\partial Y} - \frac{4}{3\,Re}\frac{\partial^2\Delta V}{\partial Y^2}\right)\Psi_V +$$

$$+ \left(\frac{1}{\rho^2}\frac{\gamma}{Re\,Pr}\frac{\partial^2\Delta e}{\partial Y^2} + \frac{4}{3\,Re}\left(\frac{\partial\Delta U}{\partial Y}\right)^2\right)\Psi_e - \frac{\kappa-1}{\rho^2}\Delta\rho\left(\frac{\partial e}{\partial Y}\Psi_V + \frac{\partial e}{\partial X}\Psi_U\right)$$

$$+ \left(\frac{2}{\rho^3}\frac{\partial P}{\partial X} - \frac{1}{\rho^3\,Re}\frac{\partial^2 U}{\partial Y^2}\right)\Delta\rho\Psi_U + \left(\frac{2}{\rho^3}\frac{\partial P}{\partial Y} - \frac{4}{3\,Re}\frac{\partial^2 V}{\partial Y^2}\right)\Delta\rho\Psi_V -$$

$$- \left(\frac{2}{\rho^3}\frac{\gamma}{Re\,Pr}\frac{\partial^2 e}{\partial Y^2} + \frac{4}{3\,Re}\left(\frac{\partial U}{\partial Y}\right)^2\right)\Delta\rho\Psi_e \qquad (27)$$

$$U\frac{\partial Q_U}{\partial X}+\frac{\partial (Q_U V)}{\partial Y}+\rho\frac{\partial Q_\rho}{\partial X}-\frac{\partial V}{\partial X}Q_V+\frac{\partial e}{\partial X}Q_e\sqrt{}+\frac{\partial}{\partial X}\sqrt{\frac{P}{\rho}}Q_e\sqrt{}+$$
$$+\frac{\partial^2}{\partial Y^2}\frac{1}{\rho\,\mathrm{Re}}Q_U\sqrt{}-\frac{\partial}{\partial Y}\sqrt{\frac{8}{3\mathrm{Re}}}\frac{\partial U}{\partial Y}Q_e\sqrt{}=$$
$$+2\Delta U\delta(X-X_m)\delta(Y-Y_m) \qquad (28)$$
$$-\Delta U\frac{\partial \Psi_U}{\partial X}-\frac{\partial(\Psi_U\Delta V)}{\partial Y}+\Delta\rho\frac{\partial \Psi_\rho}{\partial X}-\frac{\partial \Delta V}{\partial X}\Psi_V+\frac{\partial \Delta e}{\partial X}\Psi_e\sqrt{}+\frac{\partial}{\partial X}\sqrt{\frac{\Delta P}{\rho}}\sqrt{\Psi_e}\sqrt{}+$$
$$+\frac{\partial^2}{\partial Y^2}\frac{\Delta\rho}{\rho^2\,Re}\Psi_U\sqrt{}+\frac{\partial}{\partial Y}\sqrt{\frac{8}{3\,Re}}\frac{\partial \Delta U}{\partial Y}\Psi_e\sqrt{}$$

$$\frac{\partial(UQ_V)}{\partial X}+V\frac{\partial Q_V}{\partial Y}-\frac{\partial U}{\partial Y}Q_U+\frac{\partial e}{\partial Y}Q_e\sqrt{}+$$
$$+\rho\frac{\partial Q_\rho}{\partial Y}+\frac{\partial}{\partial Y}\sqrt{\frac{P}{\rho}}Q_e\sqrt{}+\frac{4}{3\,Re}\frac{\partial^2}{\partial Y^2}\sqrt{\frac{Q_V}{\rho}}\sqrt{}=$$
$$+2\Delta V\delta(X-X_m)\delta(Y-Y_m) \qquad (29)$$
$$-\frac{\partial(\Delta U\Psi_V)}{\partial X}-\Delta V\frac{\partial \Psi_V}{\partial Y}+\frac{\partial \Delta U}{\partial Y}\Psi_U+\frac{\partial \Delta e}{\partial Y}\Psi_e\sqrt{}+$$
$$-\Delta\rho\frac{\partial \Psi_\rho}{\partial Y}-\frac{\partial}{\partial Y}\sqrt{\frac{\Delta P}{\rho}}\Psi_e\sqrt{}+\frac{4}{3\mathrm{Re}}\frac{\partial^2}{\partial Y^2}\sqrt{\frac{\Psi_V\Delta\rho}{\rho^2}}\sqrt{}$$

$$\frac{\partial(UQ_e)}{\partial X}+\frac{\partial(VQ_e)}{\partial Y}-\frac{\kappa-1}{\rho}\frac{\partial \rho}{\partial Y}Q_V+\frac{\partial \rho}{\partial X}Q_U\sqrt{}-(\kappa-1)\frac{\partial U}{\partial X}+\frac{\partial V}{\partial Y}\sqrt{}Q_e+$$
$$+(\kappa-1)\frac{\partial Q_V}{\partial Y}+(\kappa-1)\frac{\partial Q_U}{\partial X}+\frac{\kappa}{Re\,Pr}\frac{\partial^2}{\partial Y^2}\sqrt{\frac{Q_e}{\rho}}\sqrt{}=$$
$$=2\Delta e\delta(X-X_m)\delta(Y-Y_m)- \qquad (30)$$
$$-\frac{\partial(\Delta U\Psi_e)}{\partial X}-\frac{\partial(\Delta V\Psi_e)}{\partial Y}+\frac{\kappa-1}{\rho}\frac{\partial \Delta\rho}{\partial Y}\Psi_V+\frac{\partial \Delta\rho}{\partial X}\Psi_U\sqrt{}+(\kappa-1)\frac{\partial \Delta U}{\partial X}+\frac{\partial \Delta V}{\partial Y}\sqrt{}\Psi_e+$$
$$-\frac{\kappa-1}{\rho^2}\frac{\partial \rho}{\partial Y}\Psi_V+\frac{\partial \rho}{\partial X}\Psi_U\sqrt{}\Delta\rho+\frac{\kappa\Delta\rho}{Re\,Pr}\frac{\partial^2}{\partial Y^2}\sqrt{\frac{\Psi_e}{\rho^2}}\sqrt{}$$

$$Q^{x=1} = 0;$$

Boundary conditions at B,C (Y=0; Y=1): $\frac{f}{fY} Q = o;$

The Hessian action on Δf_{∞} : $H(f_{\times})\Delta f_{\times} = -Q(0)$; (31)

9. Hessian spectrum bounds calculation

For obtaining the Hessian action calculation we should solve the forward, tangent linear , first order adjoint and second order adjoint problems. This is a very difficult task to accomplish from the code debugging viewpoint, and the correctness of the second order adjoint problem was not fully verified so far. Instead, the Hessian action was calculated by using the Hessian-free differentiation gradients obtained from the first order adjoint problem in the form *Hdu=(grad(u+adu)-grad(u))/a.* The codes for the forward (5-8) and first order adjoint (21-24) problems were fully verified for correctness. We used the LBFGS method of optimization [8] to perform the minimization.

The iterations $X_{m+1}=HX_m$; $\lambda=max(X_{m+1})/max(X_m)$ are used for the maximum eigenvalue calculation. The minimum eigenvalue is calculated by a method of shifted iteration [3] *(M*E-H),* where *M*- is the eigenvalues' majorant and *E* is the unit matrix.

The minimum eigenvalue is calculated also by using the Rayleigh quotient algorithm:

$R(X) = \frac{(HX, X)}{(X, X)}$; min(R(X))= λ_{min}; grad(R(X))=C(HX-R(X)X);

Iterations were performed by the steepest descent method:

$X^{k+1}=X^x-a(HX-R(X)X)$

When minimal eigenvalues are relatively large (to 10^{-3}), both algorithms present similar results (Re=10^7, λ_{min}=3.1-3.7

10^{-2}). For smaller eigenvalues the Rayleigh quotient turns out to be more accurate.

We now consider the minimum Hessian eigenvalue form the viewpoint of ill-posed problems description. Numerical results ($M=4$) demonstrated that λ_{min} is increasing as Reynolds number increases. This is connected with the changes in dissipative loss of information. (Herein, large Reynolds numbers (10^7) are formal coefficients of viscous terms). Nevertheless, the qualitative variation of the eigenvalues is correlated with the physics of the process.

Table 1

Re	100	1000	10^4	10^7
λ_{min}	$8.6\ 10^{-6}$	$5.5\ 10^{-5}$	$6.4\ 10^{-3}$	$3.4\ 10^{-2}$

The quality of the solution is also correlated to λ_{min}, (Fig.2).

Calculations were performed for estimating the variation of the λ_{min} eigenvalue with the change of scale j. The discrete wavelet transformation was used for control functions approximation.

The Daubechies-20 transformation [6] was used. The magnitude of λ_{min} (for Re=1000, M=4) for different scales is presented in Table 2.

Table 2

J	64	32	16	8
λ_{min}	$9\ 10^{-5}$	$1.5\ 10^{-4}$	$8.4\ 10^{-4}$	$9.9\ 10^{-3}$

The value of λ_{min} increases as the scale increases in accordance with results of [6]. If we chose scales j such that $\lambda_{min} \approx \sigma^2$ (where σ is the data error dispersion) we obtain a well-posed subspace of control functions. The subspaces of

smaller scales do not contain useful information and can cause the instability.

Fig. 3 presents results of all the parameters (e,ρ,U,V) ($4*64$, $N=256$ parameters) estimation ($Re=10000$) using different scales of the wavelet transformation. The instability developed from a data error $\sigma = 0.01$. Employing only 128 parameters (we neglected the detailed information of the finest scale) cured the instability. The following subspaces presented similar results. The corresponding minimum eigenvalues are presented in Table 3. The success obtained is due to the smoothness of the searched control functions. If discontinuities are present, large wavelet coefficients are present at every scale and the regularization spoils the approximation more significantly.

Table 3

J	256	128	64	32
λ_{min}	$2.8\ 10^{-4}$	$1.9\ 10^{-3}$	$1.08\ 10^{-2}$	$5.5\ 10^{-2}$

The wavelet transformation provides the parameters regularization using some physical properties of the control functions (their smallest scale, for example). It requires only about $ln(N)$ calculation of eigenvalues instead of N when the entire Hessian spectrum is used.

10. Conclusion

Numerical tests demonstrated a monotonous decreasing of the Hessian minimal eigenvalues as the scale of wavelet transformation decreases.

This new algorithm is offered for control functions' space decomposition into "well-posed" and "ill-posed" subspaces for regularization of ill-posed problems.

The algorithm is based on multiscale resolution (wavelet analysis) and Hessian minimal eigenvalue calculation using solution of the second order adjoint problem.

The schematic algorithm consists of the following stages:

1. We calculate the minimal eigenvalue of the Hessian of the cost functional. If it is greater or equal to σ^2 (σ - data error dispersion) then the problem is considered to be well-posed. If it is less σ^2 the following operations should be performed:
2. The control space is transformed into a wavelet space.
3. The detailed coefficients of the smallest scale are neglected (i.e. we are effectively decreasing the control space dimension by a factor of two).
4. Recalculate the Hessian minimal eigenvalue. If it is greater or equal to σ^2 then the problem is considered to be well-posed in this subspace. If it is less σ^2 the following scale should be neglected and the iteration is to be repeated.

Numerical tests conducted with the two-dimensional parabolized Navier-Stokes equations in the limit of large Reynolds numbers demonstrated the applicability of this algorithm to the solution of the Inverse convection problem for optimally estimating inflow parameters from down-flow data.

This new approach can be readily extended to other problems where ill-posedness is present when adjoint parameter estimation is being carried out.

References

[1] X. Zou, I.M.Navon and F.X. LeDimet, Incomplete Observations and Control of Gravity Waves in Variational Data Assimilation, Tellus, v. 44A, No 4 (1992) 273-296

[2] Liu. J, Gurrier B., Denard C., A sensitivity decomposition for regularized solution of inverse heat conduction problems by wavelets, Inverse problems, 11 (1995) 1177-1187.
[3] Zhi Wang, Navon I. M., F.X. Le Dimet and X. Zou, The Second Order Adjoint Analysis: Theory and Applications, Meteorol. Atmos. Phys., 50 (1992) 3-20.
[4] Terebigh, V.Yu., The restoration of images using minimal a priori information, Uspehi Fizicheskih Nauk, v. 165, N 2 (1995) 143-176 (in Russian).
[5] Alifanov O.M., Artyukhin E.A. and Rumyantsev S.V., Extreme Methods for Solving Ill-Posed Problems with Applications to Inverse Heat Transfer Problems, (Begell house inc. Publishers, 1996).
[6] Daubechies I, Orthonormal Basis of Compactly Supported Wavelets, Communication in Pure and Applied Mathematics, v. 41, N 7 (1988) 909-996.
[7] Le Dimet F.X., Talagrand O., Variational algorithms for analysis and assimilation of meteorological observations, *Tellus,* **38**, ser. A, N 2 (1986) 97-110
[8] Liu, D.C., Jorge Nocedal, On the Limited Memory BFGS Method for Large Scale Minimization, Mathematical Programming, 45 (1989) 503-528

Figure Captions

Fig. 1. Flow sketch. A- Entrance boundary, C-section of measurements (outflow boundary)

Fig. 2. The quality of the solution *(T(y))* for different Re (Re=10^2,10^3,10^4, 10^5 (10^5 coincides with exact)) numbers. It is correlated to λ_{min}

Fig. 3. Results of all parameters *(e,ρ,U,V)* estimation using different scales of wavelet transformation (*Re=10000*)

1-exact inflow data (*4*64, N=256*)
2- data error σ=0.01 (*N=256*)
3- first scale regularization (*N=128*)
4- second scale regularization (*N=64*)
5- third scale regularization (*N=32*)

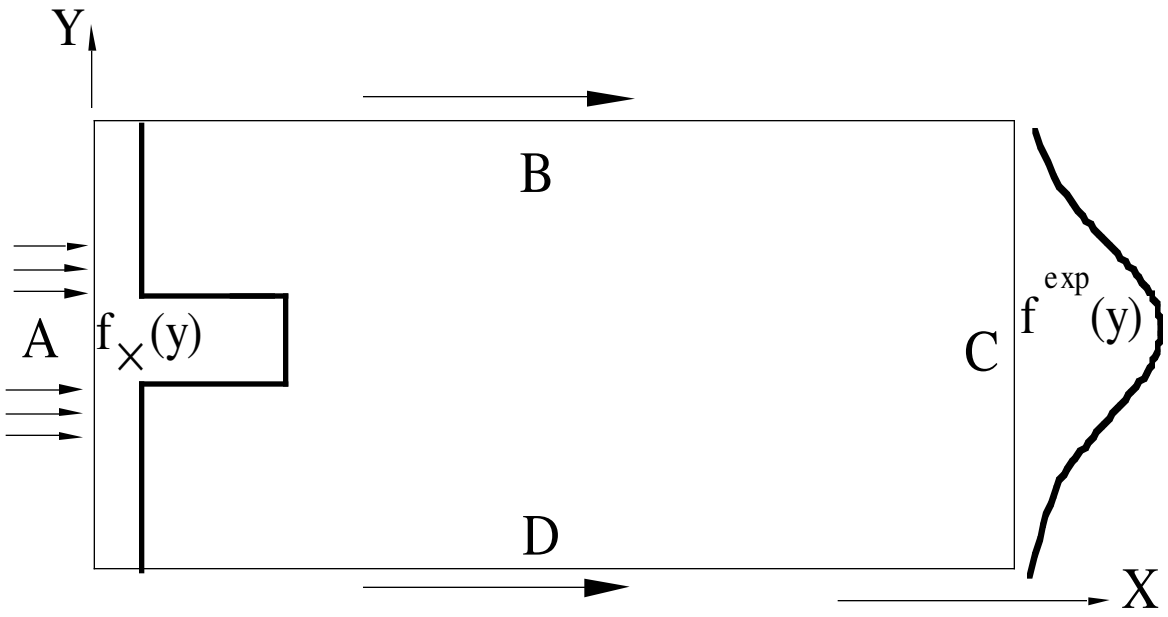

Fig. 1

Fig. 2

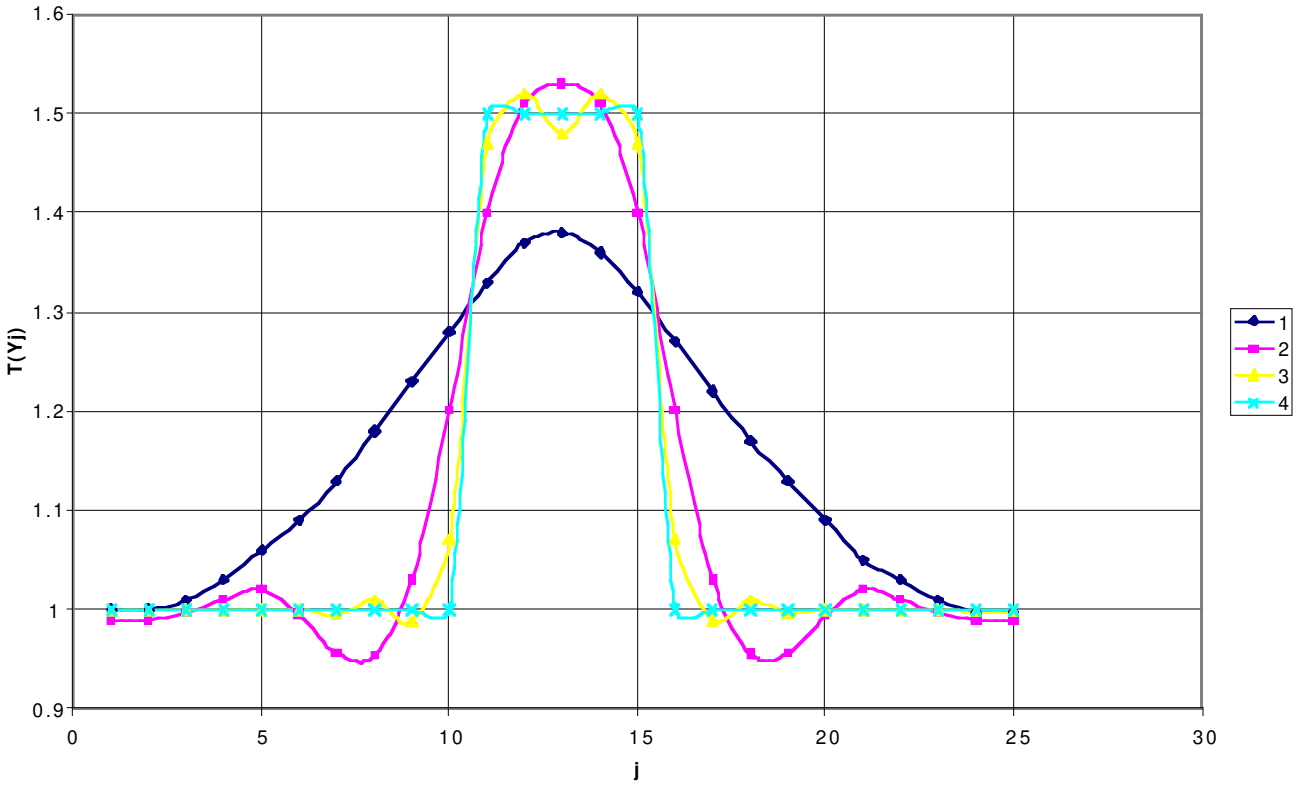

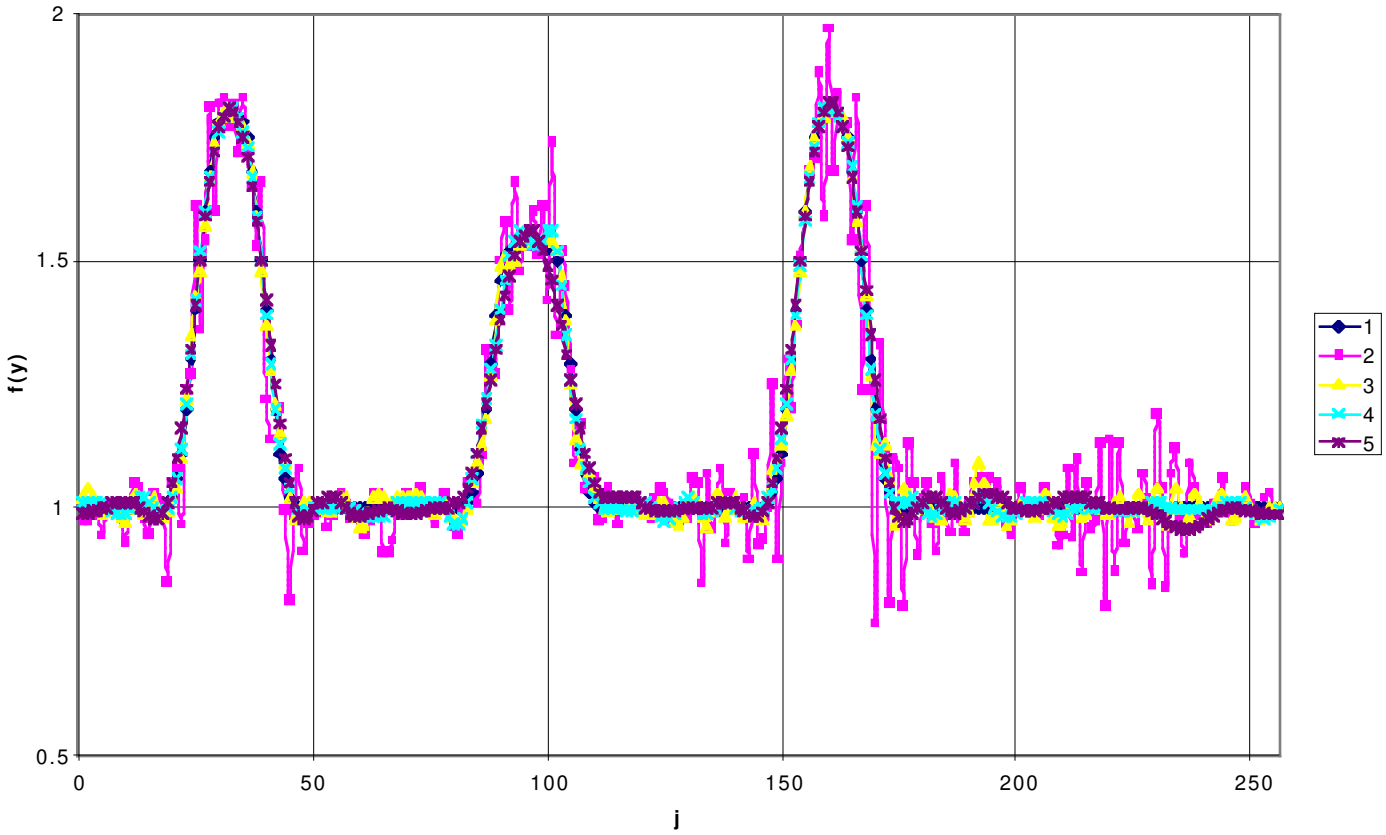
2
1.5
1
0.5
f(y)
0
50
100
150
200
250
j
1
2
3
4
5